

Generating Tunable White Light by Resonance Energy Transfer in Transparent Dye-Conjugated Metal Oxide Nanocrystals

Ting Wang, Vadim Chirmanov, Wan Hang M. Chiu, and Pavle V. Radovanovic*

Department of Chemistry, University of Waterloo, 200 University Avenue West, Waterloo, Ontario N2L 3G1, Canada

S Supporting Information

ABSTRACT: We report the design and properties of hybrid white-light-emitting nanophosphors obtained by electronic coupling of defect states in colloidal Ga₂O₃ nanocrystals emitting in blue-green with selected organic molecules emitting in orange-red. Coupling between the two components is enabled by the nanocrystal's size-dependent resonance energy transfer, allowing the photoluminescence chromaticity to be precisely tuned by changing the nanocrystal size and selecting the complementary organic dye molecule. Using this approach, we demonstrate the generation of pure white light with quantum yield of ~30%, color rendering index up to 95, and color temperature of 5500 K. These results provide a guideline for the design of a new class of hybrid white-light-emitting nanophosphors and other multifunctional nanostructures based on transparent metal oxides.

Annual global electric energy use for lighting of residential, commercial, industrial, and outdoor spaces amounts to >3400 terawatt hours and ~20% of the world's total electricity production.¹ All sources of lighting are also accountable for >1900 Mt of CO₂ emission worldwide. Conventional incandescent bulbs generally convert <5% of the consumed energy into visible light. Fluorescent lamps (FLs) and light-emitting diodes (LEDs) have emerged as energy-efficient and long-lasting lighting technologies.^{2–4} Generation of white light in these technologies relies on the phosphor conversion approach, in which multiple emission colors from phosphors and/or LEDs must be mixed in a controllable way.^{2,4} A notable example is a blue GaN-based LED coated with yellow Ce³⁺-doped Y₃Al₅O₁₂ (Ce³⁺:YAG) phosphor, in which white light is generated by mixing a portion of the blue light emitted directly by an LED with the yellow light generated by down-conversion of LED output by the converting phosphor.^{2,5} Faster and broader adoption of FLs and LEDs for general illumination applications is hampered by their design complexity and difficulties in sensitive and reproducible tuning of multicolor emission in the necessary proportion, which results in “cool” white light and/or high cost of manufacturing the devices. Subsequently, other rare earth element-based white light converters have also been developed.⁶ However, deepening concerns about the future availability of rare earth elements warrant exploring other approaches to solid-state lighting.^{7–11}

A key to overcoming these challenges is the development of efficient homogeneous phosphors capable of producing finely tuned white light that can be incorporated into lighting devices

with low manufacturing cost. Among different strategies, particular attention has been given to exploring the potential of semiconductor nanocrystals (NCs) for solid-state lighting, due to their photoluminescence (PL) efficiency, size-tunability, and compatibility with different fabrication techniques. In analogy to multi-phosphor converters, quasi-white light can be obtained by mixing NCs having different sizes,¹² or otherwise obtaining a multimodal size distribution of NCs which emit in blue, green, and red spectral regions.¹³ However, recent reports have revealed other ways of generating white light using semiconductor quantum dots, including “magic-sized” CdSe NCs, which exhibit both excitonic and surface-related emissions,⁸ and CdSe NCs fused in a silica matrix.⁹ White light has also been generated using Mn²⁺-doped CdS¹⁰ and ZnS¹⁴ NCs, which combine NC defect state and Mn²⁺ ligand field emissions, and co-doped ZnSe NCs which combine excitonic emission with emissions from multiple dopants.¹¹ While each of these approaches has some attractive aspects, in most systems discrete chromaticity values have been obtained, underscoring the difficulty in systematically generating white light. Here we demonstrate the design and preparation of white-light-emitting hybrid nanostructures with continuously tunable chromaticity, based on transparent colloidal Ga₂O₃ NCs. A unique feature of these NCs is long lifetime PL originating from electron donor–acceptor pair (DAP) recombination (hereinafter referred to as trap emission), which is sufficiently broad and size-tunable in the exact spectral region that it requires only a minor contribution to the emission from the orange-red part of the spectrum to generate white light. Motivated by these properties, we developed a class of hybrid nanophosphors in which γ -Ga₂O₃ NCs act as a primary chromophore and rationally selected dye molecules as a secondary chromophore. These systems behave as efficient single phosphors, enabling continuous tuning of the chromaticity with a high precision and homogeneity.

A series of colloidal γ -Ga₂O₃ NCs with varying average sizes were synthesized by a colloidal method, as previously described¹⁵ (see also Supporting Information (SI)). These NCs exhibit strong size-tunable PL, which has a lifetime on the millisecond time scale (Figures S1 and S2).^{15,16} The mechanism of this emission involves the recombination of an electron and a hole trapped on defect sites,¹⁶ and the emission energy can be tuned by in situ controlling defect interactions via NC size and reaction conditions.¹⁷ We hypothesized that, if we could bind to Ga₂O₃ NCs a secondary luminescent chromophore emitting in the complementary spectral range, and couple it electronically with a

Received: July 9, 2013

Published: September 18, 2013

NC, white light with desired chromaticity could be generated. A particularly promising coupling mechanism is fluorescence resonance energy transfer (FRET), which is a universal process involving transfer of the excitation energy from an electronically excited energy donor to an acceptor chromophore in the ground state.^{18,19} Furthermore, FRET has been demonstrated to be a powerful spectroscopic tool for the investigation of conjugated colloidal II–VI NCs.²⁰ The variety of available dye molecules emissive in orange-red therefore renders hybrid materials based on Ga₂O₃ NCs a promising route to obtaining white-light-emitting phosphors.

As a model system for demonstrating the utility and validity of this approach, we used Rhodamine B (RhB), which satisfies the spectral requirements and is well characterized and readily commercially available.²¹ Based on the previous studies, RhB can coordinate to Ga₂O₃ NCs via carboxylic groups by replacing TOPO ligands,²² as schematically shown in Figure 1a. The PL

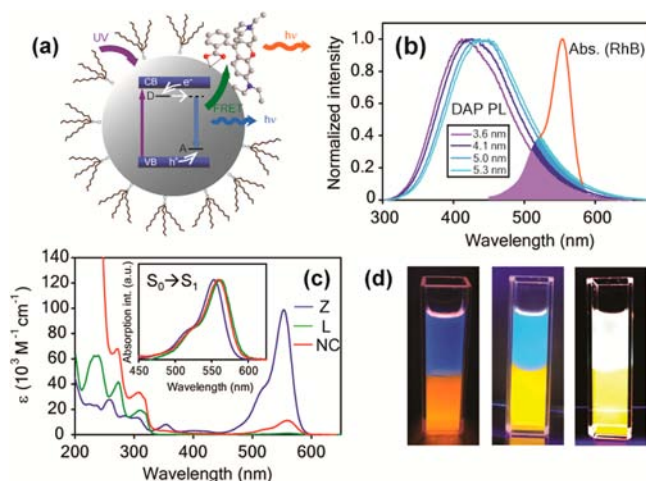


Figure 1. (a) Schematic representation of coupling between Ga₂O₃ NC and surface-bound RhB by FRET. (b) PL spectra of Ga₂O₃ NCs for different sizes ($\lambda_{\text{exc}} = 230$ nm), and absorption spectrum of RhB bound to NCs in hexane (orange). (c) Absorption spectra of RhB: Z form in water (blue), L form in hexane (green), and bound to Ga₂O₃ NCs in hexane (red). Inset: normalized $S_0 \rightarrow S_1$ absorption transitions of the same forms. (d) Photographs of PL of Ga₂O₃ NCs in hexane (top layer) in contact with RhB in water (bottom layer) over time during sample preparation.

spectra of Ga₂O₃ NCs having different sizes are shown, together with the absorption spectrum of NC-bound RhB in Figure 1b. Broadening of the Ga₂O₃ NCs trap emission band allows for partial spectral overlap between the absorption of the RhB adsorbate and the emission of Ga₂O₃ NCs. This overlap suggests the possibility of Ga₂O₃–RhB electronic coupling by FRET, given a short (≤ 5 nm) distance between PL-related NC defects, acting as FRET donors, and NC-bound RhB molecules, as FRET acceptors. Furthermore, modulation of the spectral overlap by changing NC size could enable a convenient and attractive mechanism of tuning chromaticity by changing the distribution of the PL spectral intensity. Figure 1c compares the absorption spectra of RhB in water (zwitterion (Z) form,²¹ Figure S3a) and hexane (lactone (L) form,²¹ Figure S3b) with the spectrum of RhB bound to Ga₂O₃ NCs. The L form (green) has a very different spectrum from the Z form (blue), evident by the red shift (Figure 1c, inset) and significant reduction in intensity of the $S_0 \rightarrow S_1$ band with a maximum at ~ 561 nm, which is responsible for the emission of the Z form. Consequently, RhB

(L) in hexane does not emit in orange-red. Upon transfer of RhB to a Ga₂O₃ NCs suspension, the $S_0 \rightarrow S_1$ band also experiences some red shift, and its intensity drops by a factor of ~ 9 relative to the Z form (red). These changes indicate a distinct electronic structure of RhB upon transport into nonpolar solvent containing Ga₂O₃ NCs. A decrease in the emission color intensity of RhB in water (bottom layer) and the transformation of the Ga₂O₃ NC PL from blue to white (top layer) upon excitation with 254 nm lamp during reaction (Figure 1d) suggest conjugation of NCs with RhB, consistent with our hypothesis.

The PL spectra of 3.6 nm Ga₂O₃ NCs conjugated with RhB (Ga₂O₃–RhB NCs) using different dilutions of RhB stock solution, upon excitation above the Ga₂O₃ band edge, are shown in Figure 2a. In the presence of RhB, the NC trap emission

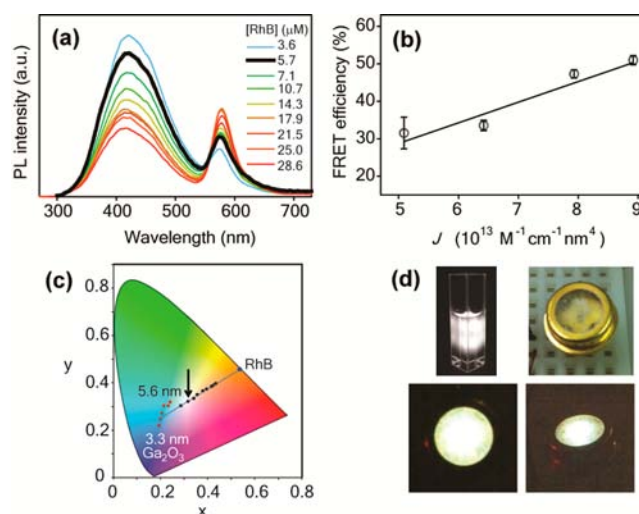


Figure 2. (a) PL spectra of 3.6 nm Ga₂O₃–RhB NCs for different concentrations of aqueous RhB, as indicated in the graph ($\lambda_{\text{exc}} = 230$ nm). Black spectrum corresponds to pure white light. (b) FRET efficiency as a function of the spectral overlap J . (c) CIE-1931 diagram corresponding to the spectra in (a) (black dots). The arrow indicates the pure white light (0.333, 0.338). The red dots designate Ga₂O₃ NCs emission color for sizes ranging from 3.3 to 5.6 nm, and the blue dot the emission of aqueous RhB solution. (d) Photographs of a colloidal suspension of white-light-emitting Ga₂O₃–RhB NCs (top left) and an LED prepared from the same sample.

quenches, while the characteristic RhB $S_1 \rightarrow S_0$ emission band appears, indicating the excitation of RhB by Ga₂O₃ NCs. Assuming the excitation of RhB by FRET, the energy transfer efficiencies (η_{FRET}) for the NC sizes in Figure 1b were calculated as $\eta_{\text{FRET}} = 1 - (F_{\text{DA}}/F_{\text{D}})$, where F_{D} and F_{DA} are relative intensities of NC trap (donor) emission in the absence and presence of conjugated RhB acceptors, respectively. For these measurements, we used the same concentration of Ga₂O₃ NCs, while the concentrations of the starting RhB solutions were adjusted to give the same optical density of the $S_0 \rightarrow S_1$ transition of RhB bound to NCs. The spectral overlap integrals $J(\lambda)$ in Figure 1b were calculated as¹⁸

$$J(\lambda) = \int_0^{\infty} F_{\text{D}}(\lambda) \epsilon_{\text{A}}(\lambda) \lambda^4 d\lambda \quad (1)$$

where $\epsilon_{\text{A}}(\lambda)$ is the extinction coefficient of RhB at wavelength λ . The FRET efficiency increases linearly as a function of the spectral overlap (Figure 2b), suggesting that RhB excitation occurs by FRET.²³ These results also suggest the possibility of generating tunable white light emission by a single wavelength

excitation, using this newly constructed hybrid emitter. Figure 2c shows a CIE-1931 chromaticity diagram indicating the color points corresponding to the spectra in Figure 2a. With increasing amount of RhB per Ga₂O₃ NC, the perceived emission color gradually transforms from deep blue to orange-red. This color transformation can be controlled with high precision and reproducibility over a wide range. We specifically highlight this point by demonstrating generation of pure white light, represented by color coordinates (0.333, 0.338), using 5.73 μM RhB solution and 3.6 nm Ga₂O₃ NCs (indicated with an arrow in Figure 2c). The white light point in the CIE-1931 diagram corresponds to the spectrum shown with a black line in Figure 2a. The colloidal suspensions of RhB-conjugated NCs are completely transparent, potentially allowing for their incorporation into transparent films and optical windows. Photographs of this white-emitting sample in colloidal form and incorporated into a LED are shown in Figure 2d (an analogous Ga₂O₃ NC-based LED is shown in Figure S4). A thin transparent layer of NCs generates bright white illumination that is sufficiently strong to be visible even in daylight. The internal quantum yield of this material is up to 30%, and is expected to be further improved primarily through an increase in the oxygen vacancy concentration in NCs,¹⁷ and through the selection of dyes with maximum efficiency. Furthermore, the color rendering index (CRI), which is used as a quantitative measure of the ability of a light source to faithfully reproduce an object color, was measured to be up to 95 for the prepared LEDs (Figure S5). This value is equal to or better than the CRI of typical FLs (80–85) measured under the same conditions with the same instrument. The correlated color temperature of this particular nanophosphor sample is ~5500 K. While the limits of long-term stability were not a focus of this conceptual study, even in a non-optimal configuration (with RhB), the nanophosphor was stable for hours of operation under low excitation power and remained active after several months.

To further study the electronic structure and properties of hybrid Ga₂O₃–RhB nanophosphor, we carried out a series of time-resolved PL measurements (Figure 3). Figure 3a compares the PL decay dynamics of RhB bound to Ga₂O₃ NCs upon excitation into the Ga₂O₃ band gap at 230 nm (black circles) and direct excitation of RhB at 563 nm (orange circles). Owing to the complete transparency of Ga₂O₃ NCs, RhB can be directly excited into S₀→S₁ transition. The resulting temporal decay was fit with a biexponential function, yielding an average lifetime ($\langle\tau\rangle$) of 3.6 ns (Figure 3b, orange circles, and Table S1). This value is larger than the lifetime of free RhB ($\tau = 1.5$ ns, green circles in Figure 3b), suggesting its reduced non-radiative decay rate, likely due to restricted molecular motion associated with binding to NC surfaces. This behavior is in stark contrast with the PL decay of RhB when Ga₂O₃–RhB NCs are excited into the Ga₂O₃ band gap (Table S1). In this case the decay rate is significantly slower, with 3 orders of magnitude longer average lifetime ($\langle\tau\rangle \approx 1.5$ μs). The extended lifetime suggests that the dynamics of RhB PL decay is determined by that of trap recombination,²⁴ and confirms that RhB is excited by FRET involving trap states in Ga₂O₃ NCs. Ga₂O₃ NC-to-RhB FRET is also evident from an increase in the decay rate of trap emission with increasing concentration of RhB attached to NCs (Figure 3c). Figure 3d shows a three-dimensional contour graph of the spectrum of colloidal Ga₂O₃–RhB NCs as a function of the delay time. The afterglow of the dual emission persists for several milliseconds after excitation, which is another favorable feature of this system. Taken together, the results of Figures 2 and 3 imply

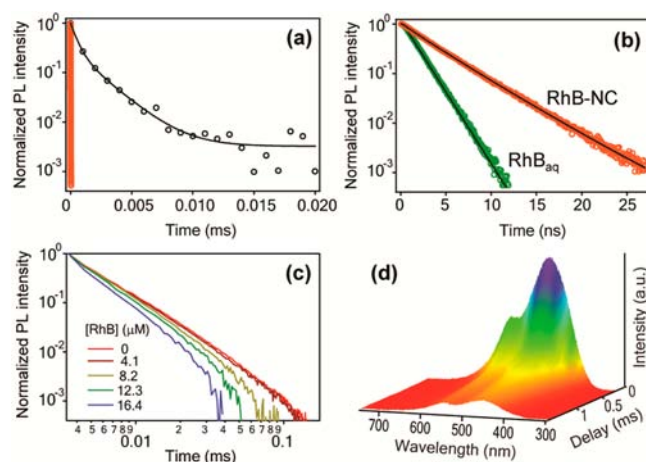


Figure 3. (a) Comparison of the PL decay of RhB bound to Ga₂O₃ NCs in hexane upon excitation of the S₀→S₁ transition at 563 nm (orange circles) and into the Ga₂O₃ NC band gap at 230 nm (black circles). (b) Comparison of the PL decay of free RhB in water (green) and bound to Ga₂O₃ NCs in hexane (orange); $\lambda_{\text{exc}} = 563$ nm. The black lines are exponential fits. (c) Time-resolved NC trap emission intensity of 5.8 nm Ga₂O₃–RhB NCs in hexane for various RhB concentrations ($\lambda_{\text{em}} = 455$ nm; $\lambda_{\text{exc}} = 230$ nm). (d) Time-gated PL spectra of 4.2 nm Ga₂O₃–RhB NCs in hexane as a function of delay (gate time, 5 ms; $\lambda_{\text{exc}} = 230$ nm).

that the Ga₂O₃–RhB hybrid system acts as coupled chromophores, allowing for the generation of homogeneous white light with tunable chromaticity and long lifetime. For further discussion see the SI. From a broader perspective, Figure 3 demonstrates effective energy storage in defect states of Ga₂O₃ NCs and its controlled release into organic adsorbates, allowing for potential applications of this nanosystem in various photonic structures and photocatalysis.

To test the generality and versatility of this hybrid approach to generating white light, and to demonstrate its potential for developing a system with optimal properties, we used ATTO 565 (A565) free carboxylic acid dye (Figure 4a) as the secondary chromophore. We chose this molecule because it has photophysical properties similar to those of RhB but is generally known to have higher thermal stability and photostability. The absorption spectrum (Figure 4b, black) confirms the presence of NC-bound A565 upon its transfer to Ga₂O₃ NCs suspension in hexane. Upon binding to NCs, A565 remains emissive, as evidenced by the characteristic PL transition following direct excitation at 557 nm (orange). Importantly, the S₀→S₁ absorption band also partly overlaps with the Ga₂O₃ NCs emission (dashed blue line), providing a mechanism for excitation by FRET. Figure 4c shows PL spectra of Ga₂O₃–A565 hybrid NCs excited into the NC band gap for different starting concentrations of A565 added to NCs suspension. A decrease in the trap emission intensity accompanied by an increase in A565 emission intensity with increasing amount of molecules per NC is consistent with the excitation of A565 by anchoring NCs. This NC-mediated excitation of A565 is confirmed by time-resolved PL measurements (Figure S6). The perceived colors associated with the spectra in Figure 4c are indicated in the CIE-1931 diagram (Figure 4d). Owing to the ability to systematically modulate spectral intensities and positions, we obtained a sample emitting pure white light by a single wavelength excitation (indicated with the arrow).

In summary, the reported results demonstrate the ability of a transparent metal oxide–organic molecule nanophosphor to

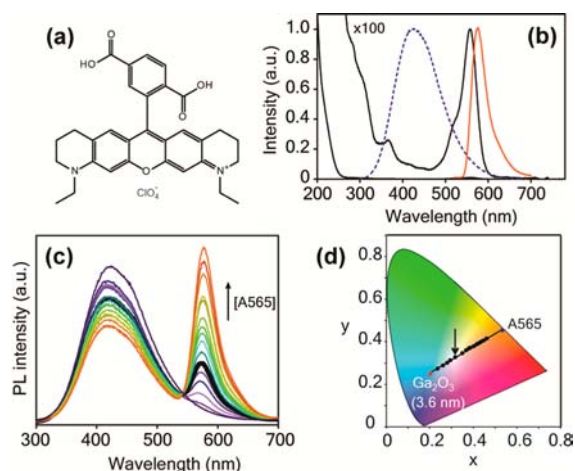


Figure 4. (a) A565 free COOH derivative perchlorate salt. (b) Absorption (black) and emission (orange) spectra of A565 bound to Ga_2O_3 NCs. The absorption spectrum is also shown multiplied by 100. The PL spectrum of Ga_2O_3 NCs (dashed blue) partially overlaps with the absorption spectrum of A565. (c) PL spectra of 3.6 nm Ga_2O_3 -A565 NCs for increasing concentrations of A565. Thicker black line corresponds to pure white light. (d) CIE-1931 diagram indicating the points corresponding to the spectra in (c). The arrow indicates chromaticity coordinates of pure white light (0.335, 0.340).

generate tunable white light by FRET. This hybrid material acts as a coupled emitter, avoiding the need for multiple phosphors or LEDs to approximate white light. Although the systems described in this report rely on UV excitation, which is more compatible with FLs than LEDs, the reported results are general and could be widely applicable for a variety of molecules and NCs. Furthermore, the colloidal form of these NCs allows for their easy manipulation using chemical means, including their incorporation into light-emitting devices. In a broader context the electronic coupling between selected molecules and functional defects in transparent metal oxide NCs could enable mutual transfer of properties of both components in the excited states, and realization of new functionalities in this class of hybrid nanostructured materials.

■ ASSOCIATED CONTENT

Supporting Information

Experimental details and further discussion; steady-state and time-resolved PL data; Z- and L-forms of RhB; photographs of blue Ga_2O_3 NC LED and CRI data (Figures S1–S6); time-decay fitting parameters (Tables S1 and S2). This material is available free of charge via the Internet at <http://pubs.acs.org>.

■ AUTHOR INFORMATION

Corresponding Author

pavler@uwaterloo.ca

Notes

The authors declare no competing financial interest.

■ ACKNOWLEDGMENTS

This work was supported by NSERC I2I and Discovery grants, C4 Consortium (PoP fund), and Ontario Ministry of Research and Innovation (Early Researcher Award to P.V.R.). P.V.R. is a Canada Research Chair. T.W. acknowledges Waterloo Institute for Nanotechnology for a Graduate Research Fellowship.

■ REFERENCES

- (1) Brown, L. R. *World on the Edge: How to Prevent Environmental and Economic Collapse*; 1st ed.; W.W. Norton & Co.: New York, NY, 2011.
- (2) Krames, M. R.; Shchekin, O. B.; Mueller-Mach, R.; Mueller, G. O.; Zhou, L.; Harbers, G.; Craford, M. G. *J. Disp. Technol.* **2007**, *3*, 160–175.
- (3) (a) Khan, N.; Abas, N. *Renew. Sust. Energ. Rev.* **2011**, *15*, 296–309. (b) Bardsley Consulting; Navigant Consulting, Inc.; Radcliffe Advisors, Inc.; SB Consulting; Solid State Lighting Services, Inc. *Solid-State Lighting Research and Development: Multi-Year Program Plan*; U.S. DOE: Washington, DC, 2012.
- (4) Smet, P. F.; Parmentier, A. B.; Poelman, D. *J. Electrochem. Soc.* **2011**, *158*, R37–R54.
- (5) Ye, S.; Xiao, F.; Pan, Y. X.; Ma, Y. Y.; Zhang, Q. Y. *Mater. Sci. Eng. R* **2010**, *71*, 1–34.
- (6) (a) Setlur, A. A.; Radkov, E. V.; Henderson, C. S.; Her, J.-H.; Srivastava, A. M.; Karkada, N.; Kishore, M. S.; Kumar, N. P.; Aesram, D.; Deshpande, A.; Kolodin, B.; Grigorov, L. S.; Happek, U. *Chem. Mater.* **2010**, *22*, 4076–4082. (b) Huang, C.-H.; Liu, W.-R.; Chen, T.-M. *J. Phys. Chem. C* **2010**, *114*, 18698–18701. (c) Dai, Q.; Foley, M. E.; Breshike, C. J.; Lita, A.; Strouse, G. F. *J. Am. Chem. Soc.* **2011**, *133*, 15475–15486. (d) Korthout, K.; Smet, P. F.; Poelman, D. *Appl. Phys. Lett.* **2011**, *98*, 261919.
- (7) (a) Kamtekar, K. T.; Monkman, A. P.; Bryce, M. R. *Adv. Mater.* **2010**, *22*, 572–582. (b) Sun, Y.; Giebink, N. C.; Kanno, H.; Ma, B.; Thompson, M. E.; Forrest, S. R. *Nature* **2006**, *440*, 908–912. (c) Zhang, Y.; Xie, C.; Su, H.; Liu, J.; Pickering, S.; Wang, Y.; Yu, W. W.; Wang, J.; Wang, Y.; Hahn, J.-i.; Dellas, N.; Mohny, S. E.; Xu, J. *Nano Lett.* **2011**, *11*, 329–332. (d) Vanithakumari, S. C.; Nanda, K. K. *Adv. Mater.* **2009**, *21*, 3581–3584. (e) Yang, Z.; Xu, J.; Wang, P.; Zhuang, X.; Pan, A.; Tong, L. *Nano Lett.* **2011**, *11*, 5085–5089. (f) Dai, J.; Ji, Y.; Xu, C. X.; Sun, X. W.; Leck, K. S.; Ju, Z. G. *Appl. Phys. Lett.* **2011**, *99*, 063112.
- (8) Bowers, M. J., II; McBride, J. R.; Rosenthal, S. J. *J. Am. Chem. Soc.* **2005**, *127*, 15378–15379.
- (9) Lita, A.; Washington, A. L., II; van de Burgt, L.; Strouse, G. F.; Stieglman, A. E. *Adv. Mater.* **2010**, *22*, 3987–3991.
- (10) Nag, A.; Sarma, D. D. *J. Phys. Chem. C* **2007**, *111*, 13641–13644.
- (11) Panda, S. K.; Hickey, S. G.; Volkan Demir, H.; Eychmuller, A. *Angew. Chem., Int. Ed.* **2011**, *50*, 4432–4436.
- (12) Nizamoglu, S.; Zengin, G.; Demir, H. V. *Appl. Phys. Lett.* **2008**, *92*, 031102.
- (13) Chen, H.-S.; Hong, H.-Y.; Kumar, R. V. *J. Mater. Chem.* **2011**, *21*, 5928–5932.
- (14) Quan, Z.; Yang, D.; Li, C.; Kong, D.; Yang, P.; Cheng, Z.; Lin, J. *Langmuir* **2009**, *25*, 10259–10262.
- (15) Wang, T.; Farvid, S. S.; Abulikemu, M.; Radovanovic, P. V. *J. Am. Chem. Soc.* **2010**, *132*, 9250–9252.
- (16) Wang, T.; Radovanovic, P. V. *J. Phys. Chem. C* **2011**, *115*, 18473–18478.
- (17) Wang, T.; Radovanovic, P. V. *Chem. Commun.* **2011**, *47*, 7161–7163.
- (18) Lakowicz, J. R. *Principles of Fluorescence Spectroscopy*, 3rd ed.; Springer: New York, 2006.
- (19) Scholes, G. D. *Annu. Rev. Phys. Chem.* **2003**, *54*, 57–87.
- (20) Halivni, S.; Sitt, A.; Hadar, I.; Banin, U. *ACS Nano* **2012**, *6*, 2758–2765.
- (21) Ramette, R. W.; Sandell, E. B. *J. Am. Chem. Soc.* **1956**, *78*, 4872–4878.
- (22) (a) Sykora, M.; Petruska, M. A.; Alstrum-Acevedo, J.; Bezel, I.; Meyer, T. J.; Klimov, V. I. *J. Am. Chem. Soc.* **2006**, *128*, 9984–9985. (b) Petruska, M.; Bartko, A. P.; Klimov, V. I. *J. Am. Chem. Soc.* **2004**, *126*, 714–715. (c) Boulesbaa, A.; Issac, A.; Stockwell, D.; Huang, Z.; Huang, J.; Guo, J.; Lian, T. *J. Am. Chem. Soc.* **2007**, *129*, 15132–15133.
- (23) Dayal, S.; Burda, C. *J. Am. Chem. Soc.* **2007**, *129*, 7977–7981.
- (24) Hegde, M.; Wang, T.; Miskovic, Z. L.; Radovanovic, P. V. *Appl. Phys. Lett.* **2012**, *100*, 141903.